Research paper

Acta Neurobiol Exp 2016, 76: 125–141

ACTA NEUROBIOLOGIÆ EXPERIMENTALIS

Surgical injury-induced early neocortical microvascular changes and characteristics of the cells populating the peri-lesion zone

Dorota Sulejczak[1], Stanisław J. Chrapusta[1], Wojciech Kozłowski[2], and Małgorzata Frontczak-Baniewicz[3]*

[1] Department of Experimental Pharmacology, Mossakowski Medical Research Centre, Polish Academy of Sciences, Warsaw, Poland, [2] Department of Pathology, Military Medicine Institute, Warsaw, Poland, [3] Electron Microscopy Platform, Mossakowski Medical Research Centre, Polish Academy of Sciences, Warsaw, Poland,

** Email: mbaniewicz@imdik.pan.pl*

Adult mammalian brain contains a number of specialized neurovascular structures termed "niches" that act as sources of neuronal cells throughout the individual's life. Some of the niches generate neurons to satisfy the need for 'replacement' neurons within the same or closely located brain structures, whereas the other can provide such cells for more distant destinations in the brain. A common characteristic of known neurovascular niches is the presence of a complex 3-dimensional network of basal lamina processes, called fractones. It apparently plays a major role in communication between the various niche-populating cell types as well as in niche activity and output. We hypothesized that similar niches may form *ad hoc* after a mechanical brain trauma, and tested this possibility in a rat model of surgical brain injury. Four days after removing a small fragment of sensorimotor cortex, the peri-wound region showed numerous symptoms of active repair and remodeling of brain parenchyma, including the presence of multiple cell types of immature phenotypes. The latter, as shown by a variety of light and electron microscopy techniques, included endothelial cell precursors as well as nestin-positive immature neural cells of astrocytic or non-glial characteristics. However, there was no evidence of *in situ* neurogenesis or a considerable migration of cells from SVZ. The centers of the said repair processes were capillary blood vessels connected with basal lamina-formed fractones. These results indicate that surgical brain trauma causes the formation of a vascular niche with no apparent neurogenic potential.

Key words: basal lamina, fractone, neocortex, neurogenesis, neurovascular niche, surgical brain injury

INTRODUCTION

Progenitor cells, due to their potential for self-renewal and production of multiple types of differentiated cells, are the cornerstones in reparative and regenerative processes. The presence of a pool of low-differentiated neural and endothelial stem cells capable of participating in these processes in adult brain has been first evidenced in two regions: the subventricular zone (SVZ) and the subgranular zone of the dentate gyrus (Gage et al. 1998, Gage 2002). More recently, several similar regions have been identified in the hypothalamus (Xu et al. 2005, Cheng 2013). The specific environment (niche) that surrounds progenitor cells residing in these zones stimulates and regulates the so-called adult neurogenesis (Alvarez-Buylla and Garcia-Verdugo 2002). The niches contain also the various components of extracellular matrix (ECM). A growing body of evidence indicates to the particular importance of endothelial cells for the existence of the niche. The assumed key role of these cells would be regulation of both angiogenesis and self-renewal and differentiation of the other niche cell populations (Riquelme et al. 2008).

A considerable fraction of niche stem/progenitor cells remains in a direct contact with the basal lamina and/or stromal cells that serve as a substrate for oriented cell division (Doetsch 2003). Basal lamina is a structure built of densely packed extracellular matrix (ECM) proteins, which affects cellular divisions and differentiation as well as developmental morphogenesis (Halfter 1998, Han et al 2009). Specific branched basal lamina formations termed fractones, which remain in contact with neural stem and progenitor cells and are likely hallmarks of neural niches, have been identified in the walls of brain lateral ventricles (Mercier et al. 2002, 2003, Kerever et al. 2007, 2015). It has also been shown that new neurovascular niches may

Received 25 January 2016, accepted 3 June 2016

Correspondence should be addressed to M. Frontczak-Baniewicz
Email: mbaniewicz@imdik.pan.pl

form in the brain in some 'tissue stress' situations, after mechanical trauma of the hypothalamus (Cheng 2013) or neocortical as well as striatal stroke (Jin et al. 2003, Ohab et al. 2006, Thored et al. 2006, Yamashita et al. 2006). In the former, new neurons can be generated locally, whereas in the latter they originate from neural stem cells migrating from SVZ into the newly formed neurovascular niche in the injury zone. Such migrating cells can be found in the respective target region already 24 h post-insult (Jin et al. 2003). The niches likely play an important role in brain parenchyma repair and/or remodeling.

We have developed a rat model intended to mimic the human clinical situation of mechanical injury of the neocortex that is a relatively frequent event during neurosurgical procedures linked to CNS tumors, malformations, hemorrhages, etc. (Frontczak-Baniewicz and Walski 2003). Our intention was to study the processes associated with the repair of the damaged brain region at different times post-injury (Frontczak-Baniewicz et al. 2011). The present study was aimed at identifying early changes following surgical brain injury (SBI), which might herald the formation of a local neurovascular niche analogous to those described by others in another brain regions. Hence we assessed the condition and morphology of blood microvessels in the peri-lesion area and characterized the cells populating this zone.

MATERIALS AND METHODS

Rats

Twenty-five adult male Wistar rats (of 200–250 g body weight at the beginning of the study) from the stock of the Mossakowski Medical Research Centre in Warsaw were used for the study. The rats were housed four to five per cage, at 12h light/12 h dark cycle (lights on at 7:00 a.m.), 22–24°C ambient temperature and 45–65% relative humidity, and were allowed free access to standard pellet rat chow and tap water. The rats were randomized between three groups:

1) rats with SBI, which were sacrificed 4 days post-lesion (n=9),
2) sham-operated rats (n=8), which were subject to all the SBI-related surgical manipulations (including opening of the meninges), except for lesioning of the neocortex, and were sacrificed 4 days later, and
3) age matched intact controls (n=8).

All efforts were made to minimize the numbers of rats used and their suffering, and all animal use procedures were in compliance with the European Communities Council Directive of 24 November 1986 (86/609/EEC) as well as with the respective Polish law regarding the care and use of laboratory animals. The experimental protocol has been accepted by the IVth Local Ethical Committee on Animal Testing at the National Medicines Institute, Warsaw, Poland (Permit No. 15/2010).

Surgical injury of the neocortex

Neocortex lesion was performed as described earlier (Frontczak-Baniewicz et al. 2011). Briefly, the rats were anesthetized with intramuscular injection of ketamine--xylazine mixture (67 and 10 mg/kg, respectively). After cutting the scalp, about 3 mm diameter portions of the right frontal bone and the underlying meninges centering 3 mm laterally from the bregma and 3 mm anteriorly to the coronal suture were removed. Next, an approximately 2×2×2 mm piece of neocortex was removed with microscissors, and the wound was covered by simple suturing of the scalp. After the surgery, the rats were returned to their normal housing under standard conditions. Additionally, they received 4 mg/kg/day of ketoprofen (s.c.) for 5 consecutive days beginning on the day of SBI.

Tissue harvesting and fixing for light and electron microscopy

All rats were deeply anesthetized with pentobarbital (80 mg/kg b.w., i.p.) and perfused by the ascending aorta, initially with 0.9% (w/v) NaCl solution in 0.01 M phosphate buffer pH 7.4 (PBS), and then with 'regular' ice-cold fixative (4% formaldehyde in 0.1 M phosphate buffer pH 7.4 – for light microscopy and electron microscopy immunocytochemistry, or with 2% paraformaldehyde and 2.5% glutaraldehyde in 0.1 M cacodylate buffer pH 7.4 – for transmission electron microscopy). Following the perfusion, the brains were removed from the skulls to be immersed for 2 h in the same fixative.

Immunohistochemistry (IHC)

The post-fixed brains meant for IHC were cryoprotected by soaking in a series (10, 20 and 30%, w/v) of sucrose solutions in PBS, and then were cut coronally into 40 µm-thick free-floating sections using a model CM 1850 UV cryostat (Leica, Germany). The sections were next incubated at room temperature for 30 min with 3% (v/v) normal goat serum solution in PBS supplemented with 0.2% (w/v) Triton X-100 (PBST) and then for 1 h at 37°C with PBST containing 1% (v/v) normal goat serum and one of the following primary antibodies (Ab):

1) anti-CD14 rabbit polyclonal Ab (Santa Cruz, Dallas, TX, USA; cat. no. 9150, dilution 1:400),
2) anti-OX43 mouse monoclonal Ab (Santa Cruz cat. no. 53109, dil. 1:400),

3) anti Flk-1 mouse monoclonal Ab (Santa Cruz cat. no. 6251, dil. 1:400),
4) anti-laminin α-2 chain rabbit polyclonal Ab (Santa Cruz cat. no. 20142, dil. 1:400),
5) anti-AC133 mouse monoclonal Ab (Abcam, Cambridge, UK, cat. no. 16518-100, dil. 1:400),
6) anti-nestin mouse monoclonal Ab (Santa Cruz cat. no. 33677, dil. 1:1000),
7) anti-GFAP mouse monoclonal Ab (Millipore, Billerica, MA, USA, cat. no. MAB3402, dil. 1:1000),
8) anti-vimentin mouse monoclonal Ab (Santa Cruz cat. no. 373717, dil. 1:400),
9) anti-doublecortin mouse monoclonal Ab (Santa Cruz cat. no. 271390, dil. 1:400),
10) anti-NeuN mouse monoclonal Ab (Millipore cat. no. MAB377, dil. 1:1000),
11) anti-CD34 mouse monoclonal Ab (Santa Cruz cat. no. 7324, dil. 1:400),
12) anti-fibronectin rabbit polyclonal Ab (Santa Cruz cat. no. 9068, dil. 1:400),
13) anti-PCNA rabbit polyclonal Ab (Abcam cat. no. ab18197, dil. 1:1000, and
14) anti-Ki67 rabbit polyclonal Ab (Abcam cat. no. ab66155, dil. 1:200).

The reaction was terminated by washing the sections with PBST. The washed sections were incubated for 1 h at 37°C with the respective secondary Ab. The secondary Abs used were as follows:

1) goat anti-mouse Ab conjugated with Alexa Fluor 594 (Molecular Probes; USA; cat. no. A11020, dil. 1:100), or
2) goat anti-rabbit Ab conjugated with Alexa Fluor 488 (Molecular Probes cat. no. A11070, dil. 1:100), or
3) goat anti-rabbit antibody conjugated with HRP (Bio Rad, USA, cat. no. 170-6515, dil. 1:1000), or goat anti-mouse antibody conjugated with HRP (Bio Rad cat. no. 170-5047, dil. 1:1000).

The formed secondary immune complexes were visualized using DAB as a chromogen. Finally, the sections were rinsed with PBST, mounted on silanized glass slides (Sigma) and coverslipped with Vectashield mounting medium (Vector Labs Inc., Burlingame, CA, USA). Immunolabeling specificity was verified by immunostaining of the respective adjacent sections with primary antibodies omitted in the incubation mixture; no immunosignal was detected in the control sections. Immunostaining was assessed with a fluorescent microscope (Nikon, Japan) and recorded with a Nikon CCD camera.

Morphology of cell nuclei was examined in microscope slides-mounted brain sections that were washed in PBS and incubated for 2 min at room temperature in Hoechst 33258 bisbenzimide dye (Sigma) solution (1 μg/ml) in PBS. The stain was then drained off and the slides were coverslipped with Vectashield mounting medium for visualization. Cell morphology was examined in microscope slide-mounted brain sections stained by standard routine hematoxylin-eosin (H&E) procedure.

Tissue preparation for ultrastructural studies

The brain samples meant for electron microscopy were dissected from the cortical region bordering the SBI site both in the injured and control (intact) rats, then were treated for few hours with the respective ice-cold perfusion medium, and finally were post-fixed in OsO_4 solution (1% w/v) in deionized water. The samples were next dehydrated with ethanol dilution series, soaked in propylene oxide, and embedded in Agar 100 resin using Agar 100 Resin Kit (Agar Scientific, Stansted, Essex, UK). Ultrathin (60 nm) sections were cut as described earlier (Frontczak-Baniewicz and Walski 2003) and examined using a model JEM-1200EX (Jeol, Japan) electron microscope.

Histological staining of transmission electron microscopy (TEM) blocks

Tissue embedded in Agar 100 resin was sectioned into 1.0 μm-thick sections using a model MT-X ultramicrotome (RMC Inc., Tucson, AZ, USA). The sections were transferred into a drop of deionized water on a glass slide, dried down in a model LKB 2208 multiplate slide warmer (Agar Scientific), and then incubated for 1–2 min with a few drops of toluidine blue stain. Next, the slides were rinsed with deionized water to remove the unbound stain, air-dried, and analyzed using a light microscope (Nikon, Japan); the images were recorded with a Nikon CCD camera.

Immunogold labeling for electron microscopy

Tissue samples were taken from rats anesthetized and perfused as above, except that only 20 ml PBS was used for the initial perfusion step (to shorten the pre-fixation time and prevent artifactual ultrastructural changes). The samples were harvested from the fronto-temporal cortex adjacent to the SBI in the lesioned rats and from the corresponding region in the intact and sham-operated rats. The samples were treated with the regular ice-cold fixative (see above) for 20 h, post-fixed in 1% (w/v) OsO_4 solution in deionized water for 30 min, dehydrated in a series of aqueous ethanol solutions, and finally embedded in Agar 100 resin. Ultrathin (60 nm) sections were cut with a diamond knife and processed by a standard post-embedding immunocytochemistry procedure. Briefly, the sections were mounted on formvar-coated nickel grids, incubated for 10 min in 10% hydrogen peroxide, washed

with water for injections and PBS (15 min each) and treated for 10 min with 1% (w/v) bovine serum albumin solution in PBS.

The primary anti-nestin antibody was the same as that used for fluorescence microscopy, except that its dilution was 1:20. The secondary antibody used was donkey anti-mouse Ab conjugated with 12 nm diameter gold particles (Jackson ImmunoResearch, PA, USA, cat. no. 70851; dil. 1:50). Specificity of immunogold labeling was verified by 'blank' staining procedure with primary antibody omitted, which resulted in no detectable staining. All immunocytochemical preparations were analyzed in a model JEM-1200EX TEM microscope.

Analysis of blood vessels in the peri-lesion zone

Cortical slices of 1 μm thickness taken from the perimeter of the wound in rats with SBI and from the respective locations in intact and sham-operated rats were stained with toluidine blue by a standard procedure. The stained slices were used for counting of blood capillaries with thickened basal lamina in seven regions of 2.5×1.5 mm size (the short side being the wound bottom) using light microscopy. Such vessels were only found in the lesioned rats. Since they showed considerable form heterogeneity suggestive of angiogenic activity in some and functional aberrations (leakiness) in the others, an additional ultrastructural analysis was performed (in 100 capillaries/rat) using TEM.

The functional status of the vessels was assessed based on their morphology. The criteria used for the assessment were as follows: 1) presence or absence of extravasated blood serum proteins and edematous astrocytic processes (with electron-light cytoplasm), and 2) presence or absence of discontinuities in the junctions between endothelial cells. New-formed capillaries were identified by vascular bridging and high hypertrophic endothelium with organelles-poor cytoplasm.

Statistics

All numerical data are shown as the mean ±S.D.

RESULTS

Morphological changes 4 days post-SBI

Morphological examination of the cortical region corresponding to the peri-SBI region showed no capillary blood vessel abnormalities and no angioblastic activity in intact or sham-operated controls. The vessels showed continuity, with no extravasated blood elements or signs of astroglia

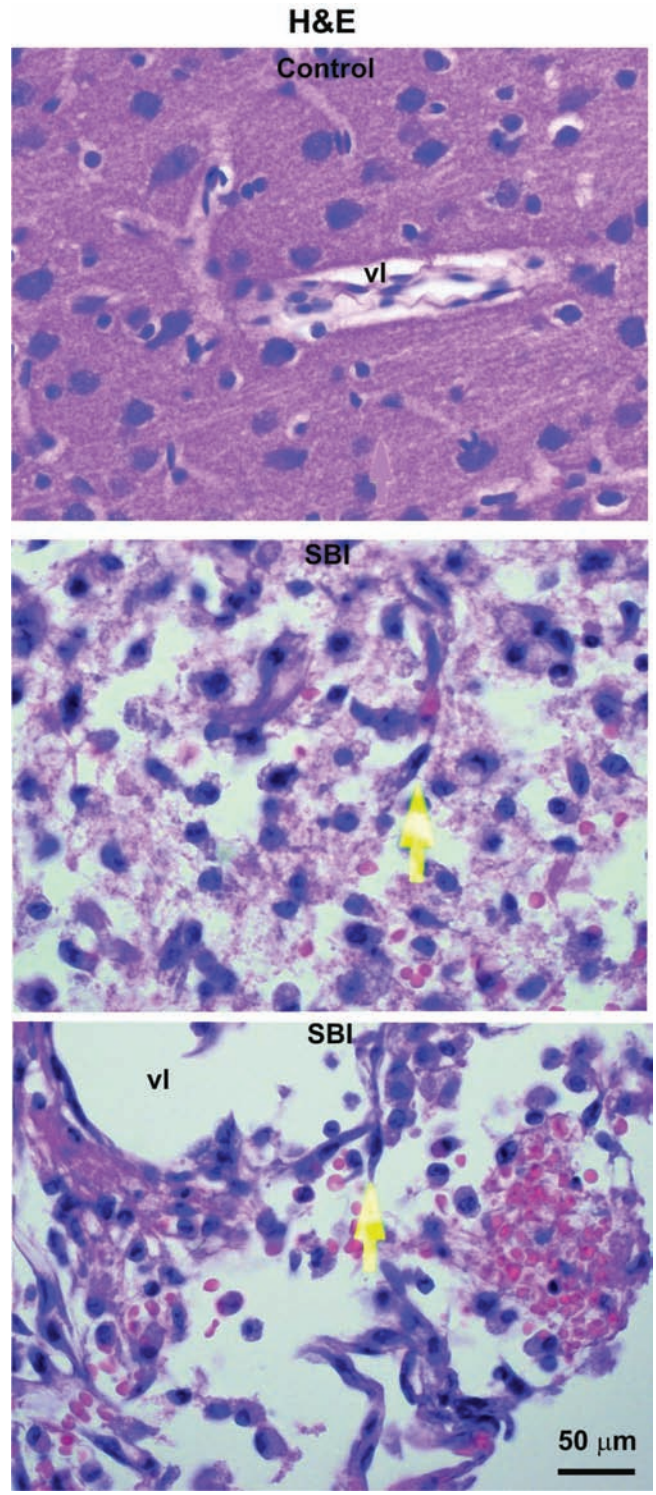

Fig. 1. Morphology of intact control and surgically injured rat neocortex; H&E staining. Control cortex (top microphotograph) shows cells and capillary blood vessels of normal appearance. The peri-wound area (middle microphotograph) shows the presence of a granulation tissue-like mass encompassing blood vessels of varying sizes. In the vicinity of some blood vessels, fusiform cells with angioblast phenotype (arrows) are seen; vl – capillary vessel lumen.

activation in their vicinity (Fig. 1). Four days post-lesion, the walls of the surgically produced cavity were lined with specific granulation tissue built mostly of granulocytes and microglia. Encompassed by the tissue were a number of angioblasts, most of which formed capillary blood vessels of varying sizes. IHC of the cells showed positive reaction for Flk-1 – the biomarker of immature endothelial cells (Fig. 2, upper panel). The peri-lesion area showed also the presence of Flk-1- and AC133-positive non-angioblast cells (possibly immature endothelial cells) in the vessel walls (Fig. 3). Some of the blood vessels present inside the granulocytic-astroglial mass showed wall discontinuity. The studied region showed also multiple occurrences of blood extravasation, mostly in a close vicinity of the blood vessels. At the perimeter of the 'granulation tissue', i.e., at the points of contact with normal brain parenchyma, abundant hypertrophied astroglial cells were apparent (Fig. 4). Neither angioblastoid cells nor the signs of astroglia activation were seen in the cortex of intact or sham-operated rats (Figs 1 and 2).

Post-SBI vasculature changes (angiogenesis)

Toluidine blue staining of the peri-SBI region revealed the presence of multiple blood vessels (5.8±1.5 vessel/mm^2) covered by thickened basal lamina occasionally connected

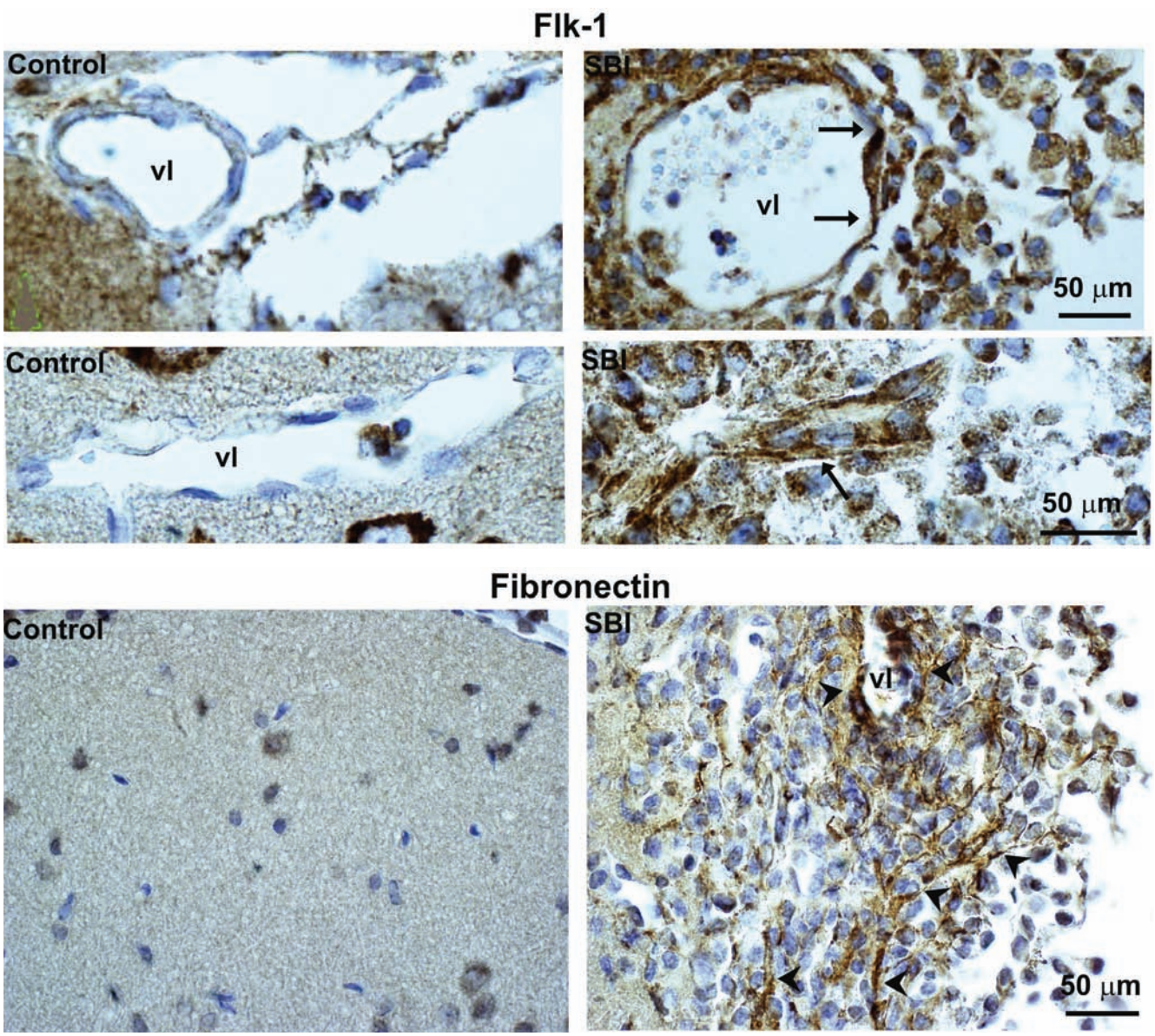

Fig. 2. Flk-1 (upper panel) and fibronectin (bottom panel) immunoreactivity (IR) in intact control and surgically injured rat neocortex. The control samples reveal no or occasional blood vessels with weak Flk-1 IR and no fibronectin-positive fibers. The peri-SBI region shows the presence of capillary blood vessels with clear wall Flk-1 IR (arrow) and numerous fibronectin-positive fibers (arrowheads); vl – capillary vessel lumen.

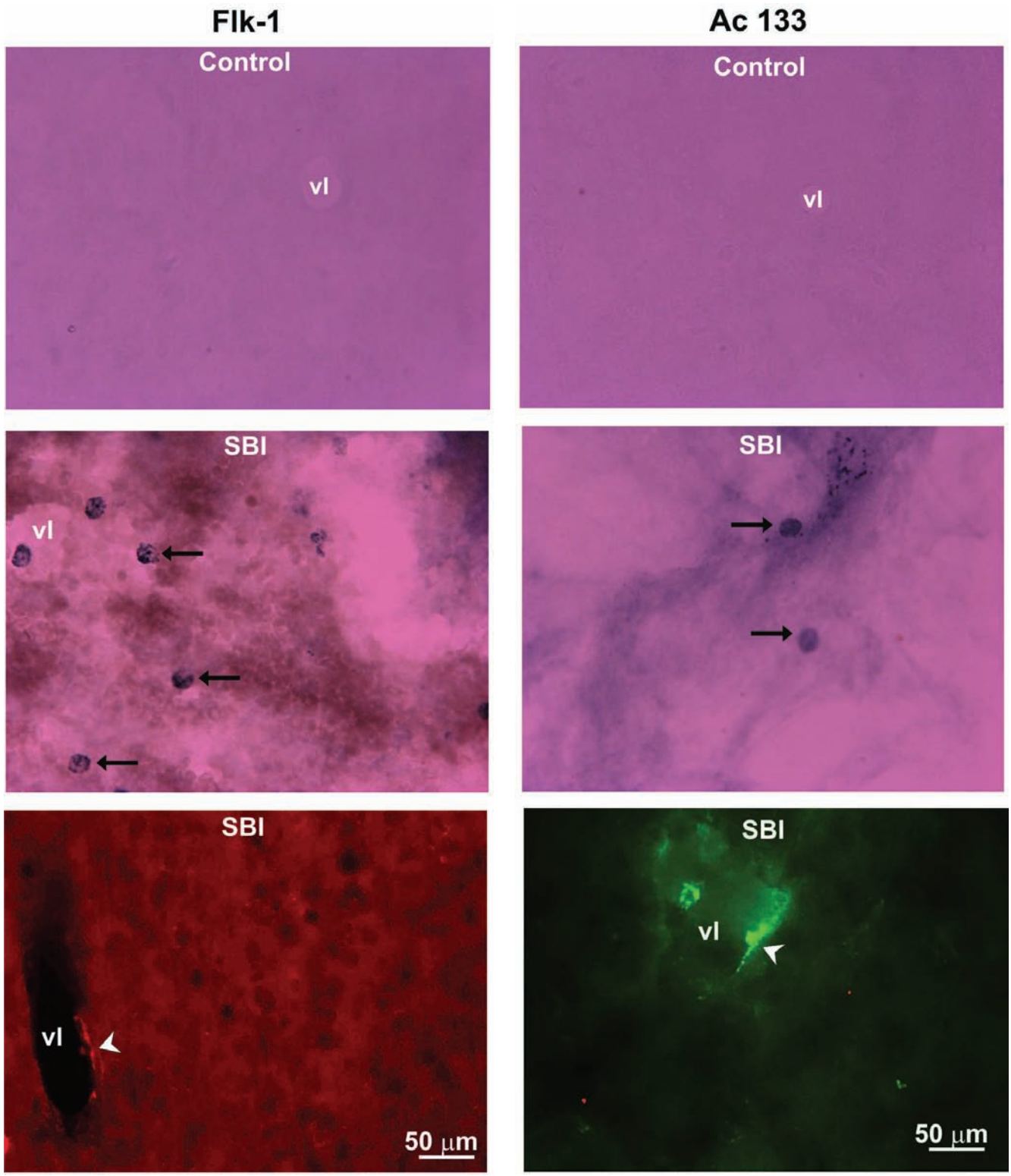

Fig. 3. Cortical sections immunostained for Flk-1 and AC133. No Flk-1 or AC133 staining was detected in intact controls (upper panels) or sham controls (not shown). Left panels show Flk-1 IR visualized by DAB (middle microphotograph) or Alexa Fluor 594 (bottom microphotograph). Right panels show AC133 IR visualized by DAB (middle microphotograph) or Alexa Fluor 488 (bottom microphotograph). Please note the presence of Flk-1- and AC133-immunopositive cells (arrows) and capillary blood vessels (arrowheads) within the peri-SBI area; vl – capillary vessel lumen.

with fractone-like structures. The branches encompassed neurons, astrocytes and cells with phenotypes indicative of haematopoietic origin as assessed by cell and nucleus shapes and the presence of cytoplasmic granules (Fig. 5). IHC staining demonstrated that the vessels were surrounded by fibronectin- (a basal lamina and ECM component) -positive fibrillary formations intermingled with microglia and astrocytes (Fig. 2, lower panel). No such fibers were found in the intact and sham-operated controls. Some of the atypical capillaries showed signs of bridging, leakiness and/or perivascular edema. These observations were next confirmed by TEM using tissue blocks from the same peri-SBI regions. These vessels showed also a considerable morphological heterogeneity. A majority of them (72.2±7.7%) showed signs of leaking, whereas another major fraction (24.4±7.6%) revealed no leakiness, but clear symptoms of angiogenesis (see Fig. 6, upper and lower panel, respectively). The remaining vessels (3.4±1.0%) showed the presence of fractone-like multiple appendices of the basal lamina invading brain parenchyma at the wound perimeter (Figs 7 and 8). These structures were interspaced with cells of varying ultrastructural morphology, including that of monocytes, granulocytes, lymphocytes, macrophages, pericytes and microglia. Astrocytes, neurons and endothelial cells with mature and immature phenotypes were apparent as well, some of which were apparently dying (not shown) or in the process of cell division (Fig. 7). However, the vicinity of the fractones showed no massive neurogenesis or cells with nuclear localization of either Ki-67 or PCNA (established markers of dividing cells; data not shown).

Immunhistochemistry of the peri-SBI region

The identity of the cells listed above was verified with further IHC studies, including a search for laminin positivity in blood vessels. The vicinity of blood vessels in the injury zone as well as the walls and the lumen of the vessels showed the presence of cells that were positive for the markers typical of the common precursors of the hematopoietic cell line and of endothelial cells, namely CD14, CD34 and OX43 (the latter considered a marker of rat vascular endothelium cells).

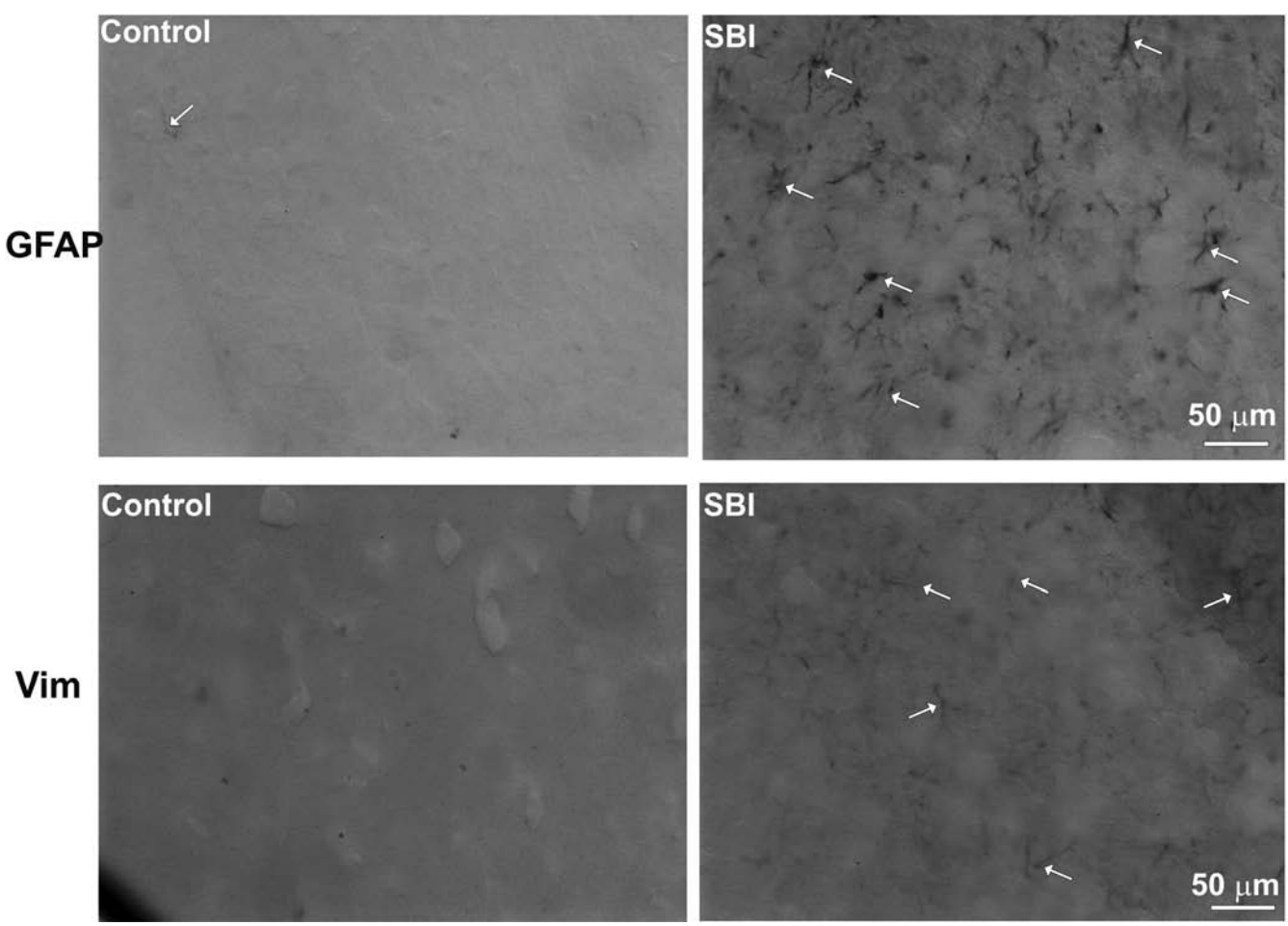

Fig. 4. GFAP (upper panel) and vimentin (lower panel) immunolabeling of neocortical astrocytes in intact controls and in SBI rats. Arrows indicate immunopositive cells. Note markedly elevated numbers of IR-cells and IR-intensity in the SBI rats.

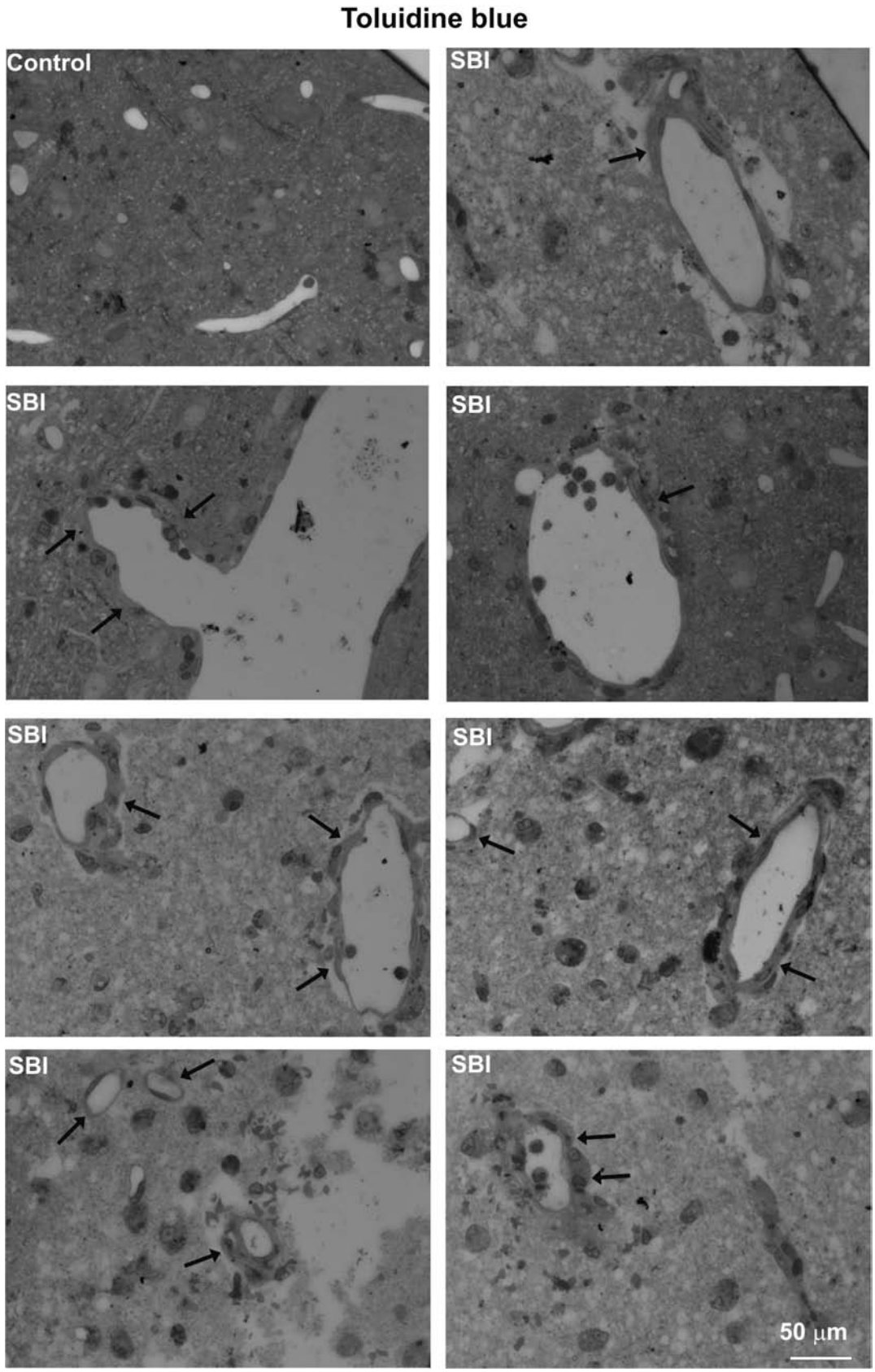

Fig. 5. The effect of SBI on blood vessel and basal lamina appearance (toluidine blue staining). Note marked thickening (arrows) of the basal lamina in SBI rats.

CD14 protein acts as a co-receptor for the lipopolysaccharide that is the major component of the outer cell membrane of Gram-negative bacteria; this receptor is found mainly in macrophages, monocytes, dendritic cells and endothelial cells. Our studies revealed a weak CD14 expression in some brain cortex vessels in control rats, and much stronger expression, both in terms of staining intensity and positive cell count, in the peri-wound zone in the rats with SBI. CD14 immunopositivity has also been observed in the cells present inside the blood vessel lumen and in the brain parenchyma in the vicinity of the peri-wound vessels (Fig. 9, left panel). Similar results were obtained for OX43. Intact and sham-operated rats showed but a low intensity vascular OX43 immunostaining, whereas much stronger OX43 staining was found in the cortical vessels of rats with SBI. OX43-positive cells were also seen in the lumen of the blood vessels and in the adjacent brain parenchyma. Double immunostaining revealed co-expression of CD14 and OX43 in all the three locations: within blood vessel walls and in blood vessel lumen as well as in brain parenchyma (Fig. 9, left panel).

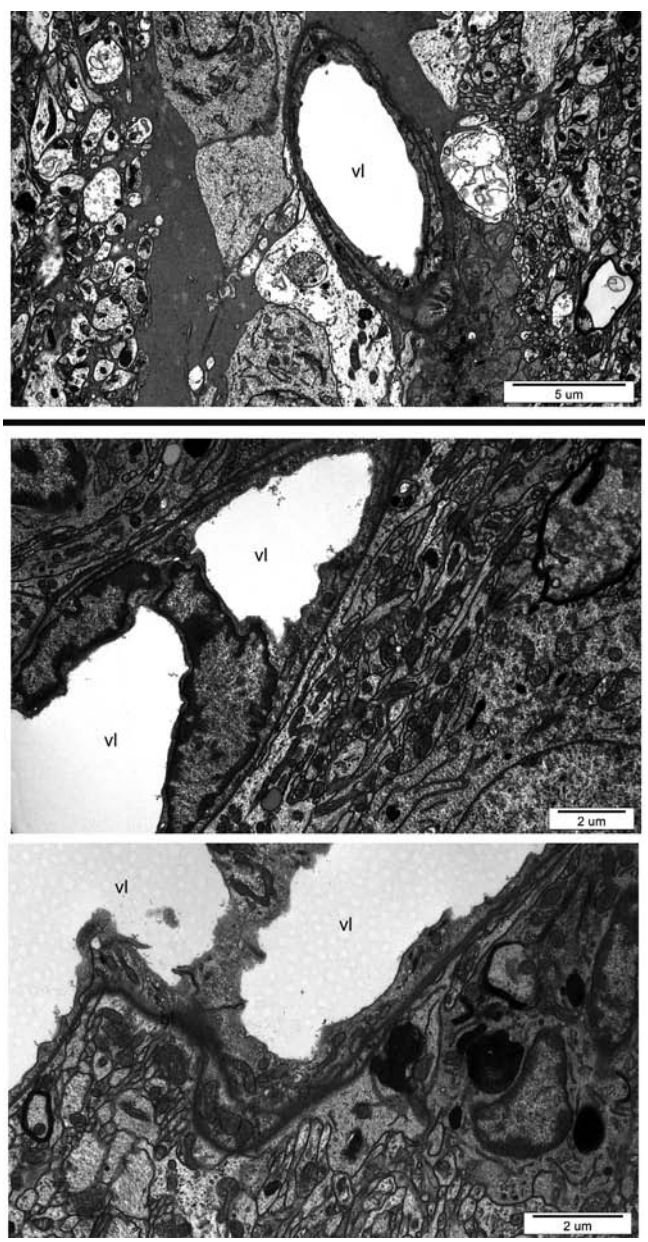

Fig. 6. Ultrastructure of peri-SBI capillaries with thickened basal lamina. Upper panel shows a vessel with leakage symptoms. Lower panel shows vessels with symptoms of angiogenesis; bl – basal lamina, vl – capillary vessel lumen.

CD34 is a marker of mesenchymal stem cells (MSC) and progenitor endothelial cells. Brain cortex from intact and sham-operated rats showed low levels of CD34 immunostaining in blood vessel walls. CD34 positivity was much stronger and the number of CD34-positive blood vessels was considerably higher in the peri-SBI cortex of lesioned rats (Fig. 9, right panel). In the latter, CD34-positive cells were also found in the vessel lumen and the adjacent brain parenchyma. Laminin, the marker of ECM, was present in the basal lamina of blood vessels as well. Intact and sham-operated rats showed a moderate laminin immunostaining around the blood vessels in the studied brain cortex region. Rats with SBI showed markedly higher level of the staining in the blood vessels in the immediate vicinity of the lesion (Fig. 8, right panel). Besides ample fibronectin immunostaining, the peri-SBI zone showed the presence of abundant laminin-positive fibrillary structures. Double immunostaining has demonstrated that signals for CD34 and laminin colocalized within blood vessels. The rats with SBI showed blood vessels with strong CD34 staining in the thick laminin-positive stroma.

Immature cells within peri-SBI area

Beginning shortly after the SBI, the peri-wound zone showed also infiltration of cells with the phenotype of immature neural cells, mostly near normal-looking novel blood vessels. Immunochemistry demonstrated the presence of nestin-positive cells, some of which were morphologically close to astrocytes, whereas the others showed non-glial characteristics (Figs 10 and 11, upper panels). The vicinity of blood vessels in the peri-wound zone showed also the presence of few doublecortin- (DCX) -positive cells (Fig. 10, lower panel), whereas no DCX- or nestin-positive cells were seen in the brain parenchyma of intact and sham-operated controls. The cortical region adjacent to the injury revealed the presence of many atypical cells resembling neither immature brain nor blood cells (Fig. 11, lower panel). The phenotype of these cells indicated that they were immature endothelial cells that, as shown by our previous investigations, will give rise to new capillaries in the peri-lesion area within next few days. However, there was no sizable cell infiltration from the SVZ into the peri-SBI zone.

DISCUSSION

Insults to brain parenchyma induce a complex response including a variety of intercellular interactions. The peri-wound zone is an arena for two concurrent while opposing types of insult-related phenomena: one resulting in cell death, destruction of brain parenchyma and the emergence of inflammatory response, and the consequential expansion of the damage. The other type is aimed at the promotion of cell survival and reconstruction

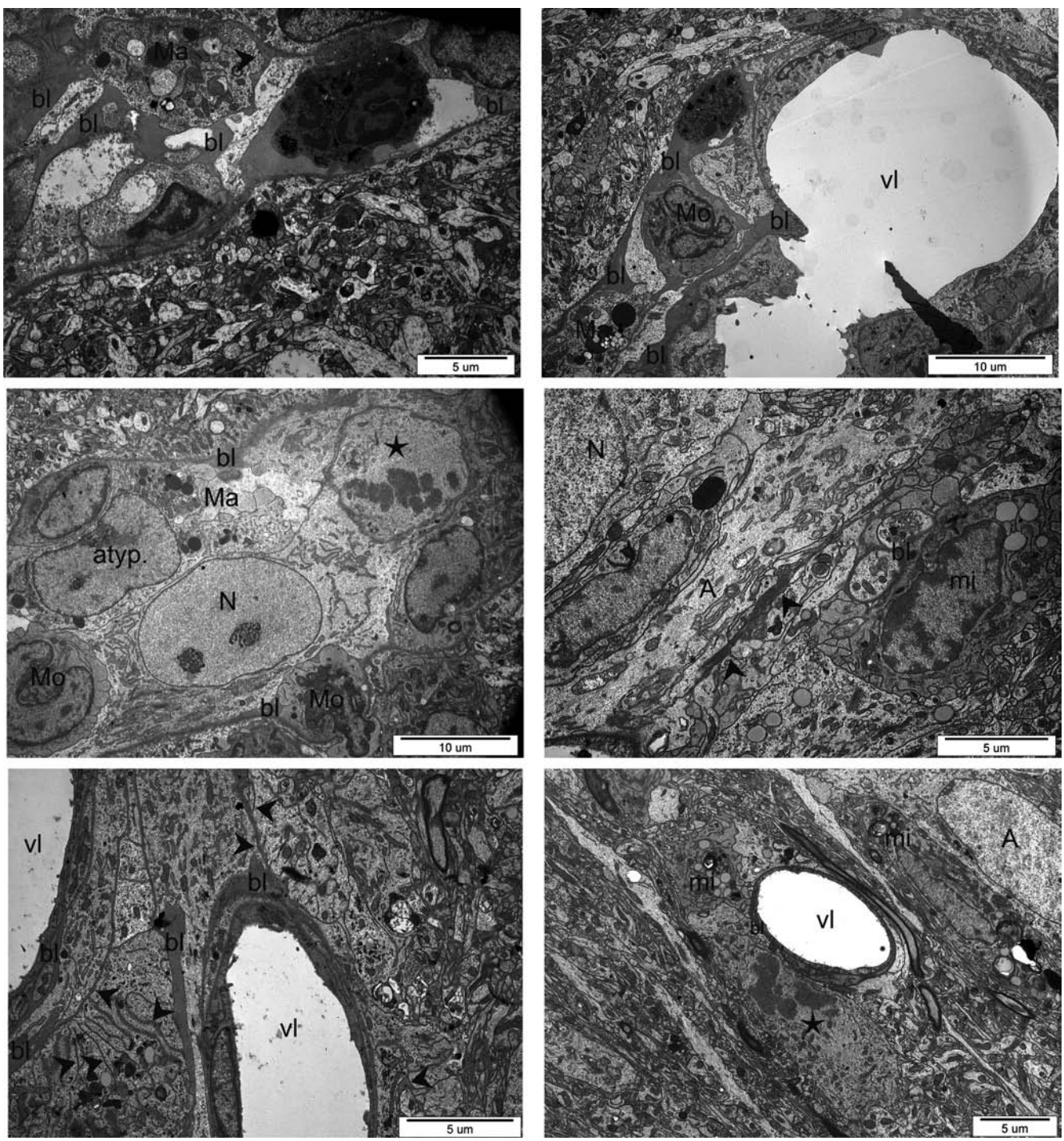

Fig. 7. Ultrastructure of peri-SBI cortex. Wound perimeter shows the presence of numerous capillary vessels encompassed by thickened basal lamina (bl). The fractone (arrowheads) network contains cells with morphological characteristics of astrocytes (A), neurons (N), microglia (mi), monocytes (Mo) and macrophages (Ma), as well as cells of atypical morphology (atyp); vl – capillary vessel lumen. In the vicinity of the fractones, dividing cells with visible chromosomes (asterisks) are seen.

of the damaged parenchyma zone. The results of this study indicate that the healing-related phenomena involve stem and progenitor cells residing in both the SVZ and brain parenchyma.

Our present data show that SBI results in a massive neurodegeneration associated with subsequent inflammatory phenomena involving microglia activation and astrogliosis that take place over a few days after the injury, and are in line with earlier reports (del Zoppo et al. 2007, Ito et al. 2007, Sulejczak et al. 2008). Neurons in the damage zone die either by necrosis (mainly during the first post-SBI day) or by apoptosis (Sulejczak et al. 2008). However, our earlier data revealed also that some neurons in the peri-SBI region survive. These cells, in contrast to the dying ones, showed an abundance of the vascular endothelial growth factor (VEGF) receptor Flk-1, which is characteristic of endothelial cells forming new capillaries (Rosenstein and Krum 2004). Besides dying neurons, the peri-SBI area showed the presence of (less numerous) dying astrocytes, but the latter were clearly outnumbered by activated astrocytes (Sulejczak et al. 2008). It is known that astrocytes are essential for neuron survival (Domingues et al. 2010).

Brain trauma usually causes permeabilization of the blood-brain barrier, which phenomenon is evidenced by numerous ultrastructural studies (Nag et al. 1997, Nag 2003, Lossinsky and Shivers 2004, Nag et al. 2009). Plasma transudation into the brain parenchyma results in a massive influx of, inter alia, albumins, fibronectin

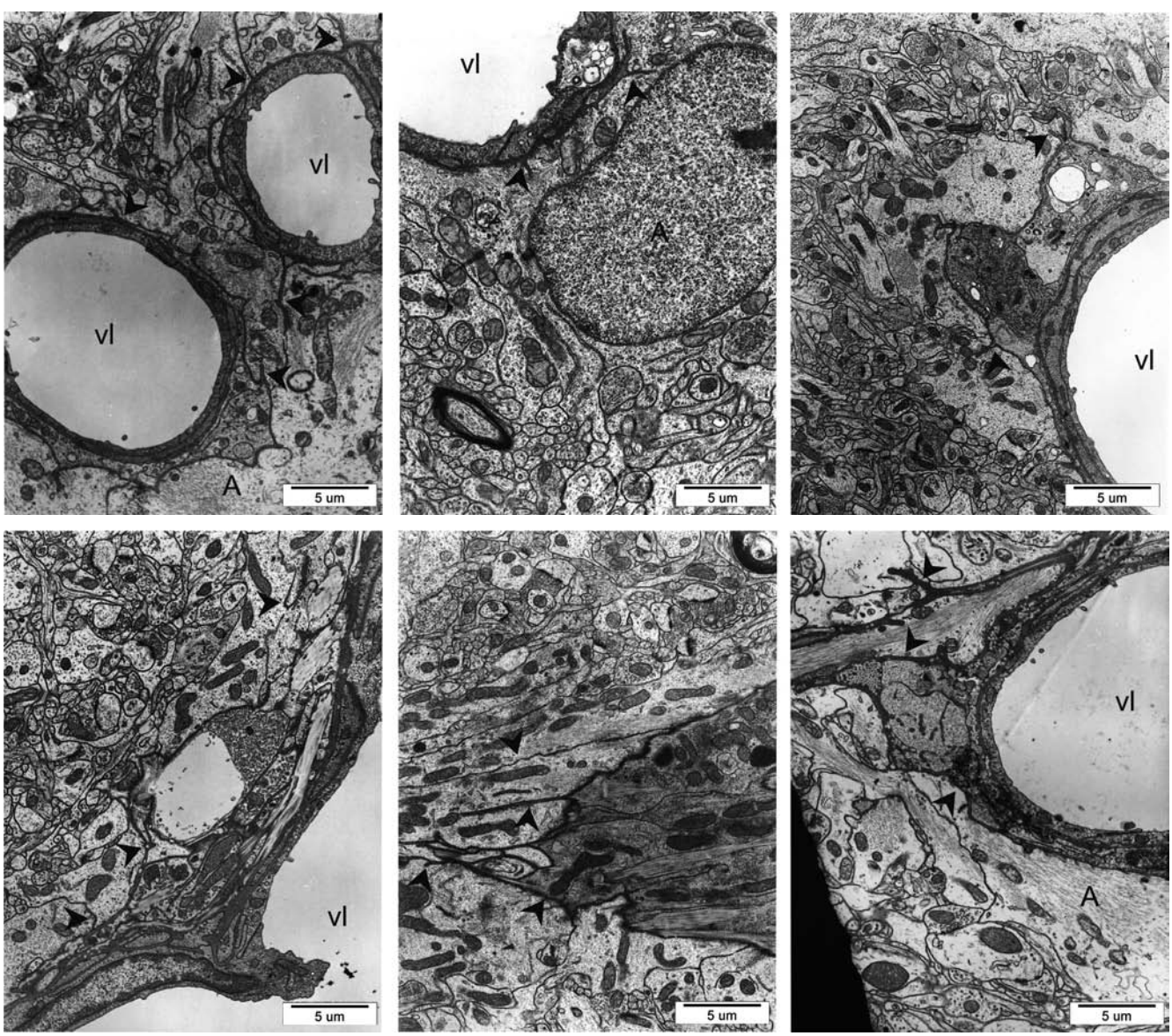

Fig. 8. Representative electronograms showing the presence of variably shaped fractone-like appendices of the basal lamina invading brain parenchyma at the perimeter of the SBI (arrowheads); A – astrocyte, vl – blood vessel.

and fibrinogen (Nag 2002), and the emergence of brain edema. In our model, the border zone of the SBI revealed an early perivascular astrocytic edema and infiltration of leukocytes and other blood cells, whereas endothelial cells showed increased numbers of pinocytic vesicles, but no clear ultrastructural symptoms of damage. The developing edema resulted in capillary damage, including failure of tight junctions.

The present data extend our previous findings regarding the angiogenesis in the peri-SBI region during the early post-injury period, which demonstrated that the wound perimeter regions filled with extravasated proteins were densely populated by clustered immature endothelial cells. Those observations suggested infiltration of the cells with the extravasated blood (Frontczak-Baniewicz and Walski 2003, Walski and Frontczak-Baniewicz 2003,

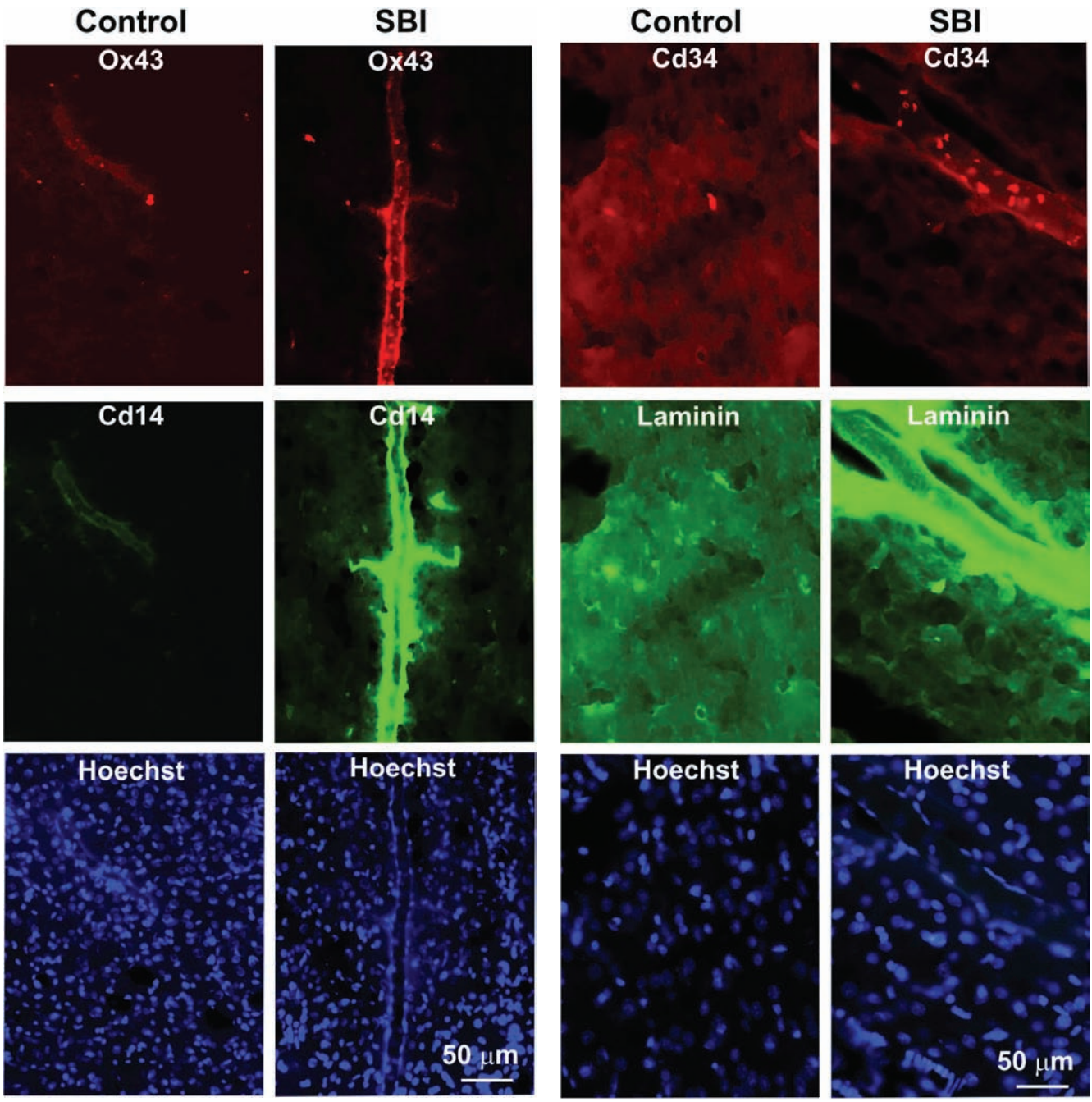

Fig. 9. Double immunofluorescence staining (top and middle microphotographs: OX43/CD14 – left panel, CD34/laminin – right panel) of the neocortex in the intact controls and SBI rats. Note the co-localization of the 'paired' markers in some cells or blood vessels, and marked enhancement of the immunostaining in SBI rats. Bottom microphotographs show fluorescent dye Hoechst 33258 staining of cell nuclei.

Frontczak-Baniewicz et al. 2007). In this study, we have found that this region also harbors cells with angioblast phenotype. Angiogenesis was also observed in other models of traumatic brain injury (Morgan et al. 2007), as well as in brain ischemia (Fan and Yang 2007). The formation of novel capillaries is associated with an increased permeability of the walls of pre-existing capillaries and the resultant increase in extravasation of plasma proteins that likely form a scaffold for the new vessels (Dvorak et al. 1995). The plasma proteins-filled peri-SBI region revealed also the presence of degenerating and dying neurons and edematous astrocytes. The plasma proteins likely were taking part in the formation of new capillaries, as they encompassed clusters of cells with ultrastructural characteristics of juvenile-looking atypical endothelial cells characterized by the presence of intracytoplasmic filaments of about 5 nm diameter. These cells took part in the formation of new vessels and co-existed with cells showing some neural precursor characteristics, namely nestin and DCX positivity.

Surprisingly, whereas angiogenesis begins already few hours post-SBI (Frontczak-Baniewicz and Walski 2006), only a minor fraction of the newly formed capillaries showed the attributes of finished, ultrastructurally normal blood vessels surrounded by astrocytic processes 4 days post-injury. A majority of the novel vessels, in spite of their proximity to ultrastructurally normal endothelial cells, pericytes, astrocytes and neurons, lacked a regular basal lamina and were embedded in an amorphous basal lamina-like material instead. Another major fraction of the novel capillaries formed in the zone of SBI and its immediate vicinity showed additional endothelial hyperplasia and absence of pericytes at the vessel wall. The workability of such vessels is in serious doubt (Frontczak-Baniewicz and Walski 2006), as vascular network function requires not only endothelial maturity, but also a functioning pericyte-endothelial cell linkage. Pericytes participate in the regulation of proliferation, migration, survival and differentiation of endothelial cells, and possibly also of blood flow and vessel wall permeability (Carmeliet 2003). According to some data, the pericytic network may also be a specific stem cells' niche (Corselli et al. 2010). The peri-SBI zone showed also infiltration of immature endothelial cells from pre-existing blood vessels. The origin of these cells was evidenced by their presence in both the walls and

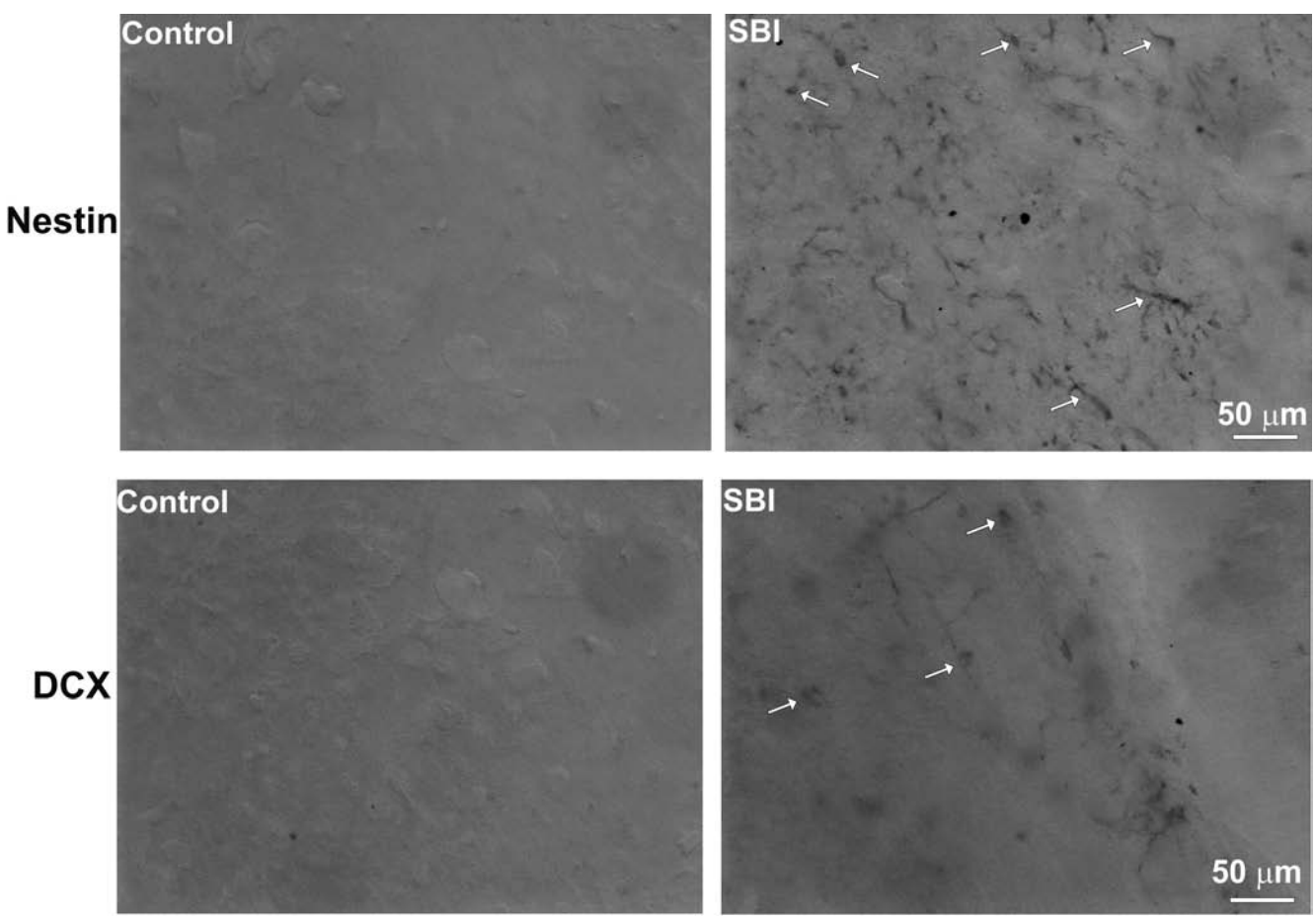

Fig. 10. Nestin (upper panel) and doublecortin (DCX, lower panel) immunolabeling of neocortical cells (arrows) in the intact control and SBI rats. Note the absence of IR cells in the intact cortex and the morphological heterogeneity of nestin-IR cell population in the SBI rat.

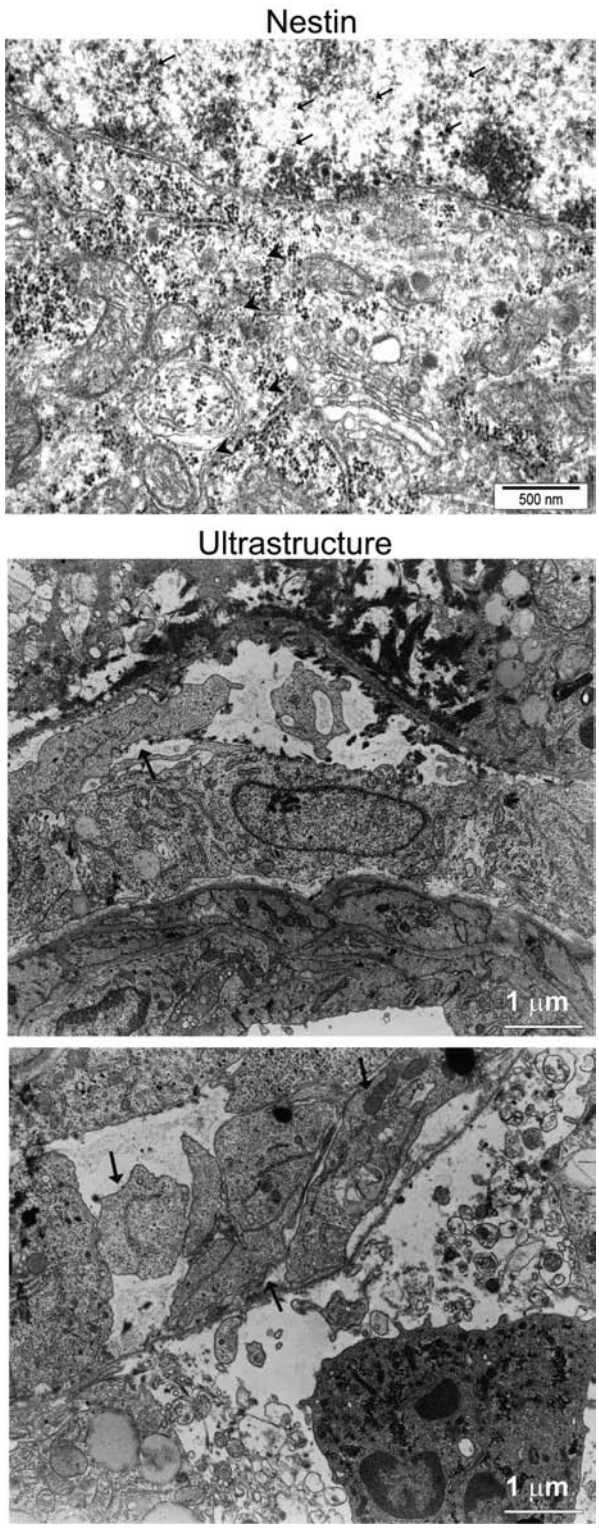

Fig. 11. Electron microscopy of injured cerebral cortex. Top microphotograph shows immunogold labeling for nestin. Note neuronal subcellular localization of nestin-bound immunogold in the injured cortex. Arrows show nuclear localization of nestin-bound immunogold particles; arrowheads point at cytoplasmic nestin-bound immunogold particles. Ultrastructure of the peri-wound neocortex (middle and bottom microphotographs) reveals the presence of atypical cells (arrows) with organella-poor cytoplasm.

lumen of the vessels (Frontczak-Baniewicz and Walski 2006). Yet another source of the cells might have been resident stem/progenitor cells of the brain parenchyma (pericytes or mesenchymal stem cells) that were activated after the SBI and were induced to proliferate at the injury site (Corselli et al. 2010).

Marked *in vitro* heterogeneity of circulating endothelial progenitor cells became the basis for the proposal that the various subsets of these cells may play diverse roles in angiogenesis (Hur et al. 2004). However, the results of our studies presented above suggest that SBI provides an impulse for the formation of new vessel from progenitor cells, and that the apparent diversity of the progenitors represents the various stages of their differentiation. Notably, EPC differentiation spans the period of about two weeks (Peichev et al. 2000). Based on our studies, we believe that the injury zone remains the scene of continuing remodeling of the capillary network for at least few weeks, resulting in enduring presence of a large number of immature-looking microvessels in the peri-SBI zone.

Post-trauma neurogenesis in the brain cortex of adult mammals is given an increasing attention (Gu et al. 2000, Jiang et al. 2001, Jin et al. 2003, Sundholm-Peters et al. 2005, Ohira et al. 2010). Most recent data not only evidence an influx to the traumatized region of immature neural cells from the SVZ and dentate gyrus, but also indicate to a possibility for *in situ* neurogenesis in the peri-injury zone. For instance, a slight induction of neurogenesis in the neocortical layer 1 of adult rats was observed after mild global forebrain ischemia (Ohira et al. 2010). Interestingly, those authors reported also the presence of single cells with neural stem cell/neuronal progenitor cell phenotype in the neocortex of control (ischemia-unaffected) brains. These findings clearly warrant further studies on adult brain neurogenesis.

The aim of this study was to investigate the possibility of formation, in the peri-SBI region of brain neocortex, of neurogenesis-promoting zones. Based on our knowledge of the structure of neurovascular niches, we looked for such zones near capillary blood vessels. The essential features of the sought-after structures included the presence of branched ECM framework as well as of immature cells with phenotypes conforming to those of progenitors/precursors of the various cell types forming brain neocortex.

Our data demonstrate that the vicinity of properly formed blood vessels in the peri-SBI zone was populated also by immature non-endothelial cells. Shortly after the lesion, cells with features of immature neural cells appeared in the peri-lesion zone, which were nestin-positive and showed either astrocytic or non-glial characteristics. Our studies have also shown the emergence of cells expressing the marker of migrating juvenile neurons DCX. We suppose that both the nestin-positive and DCX-positive cells arrived from SVZ and participated in either the restoration of

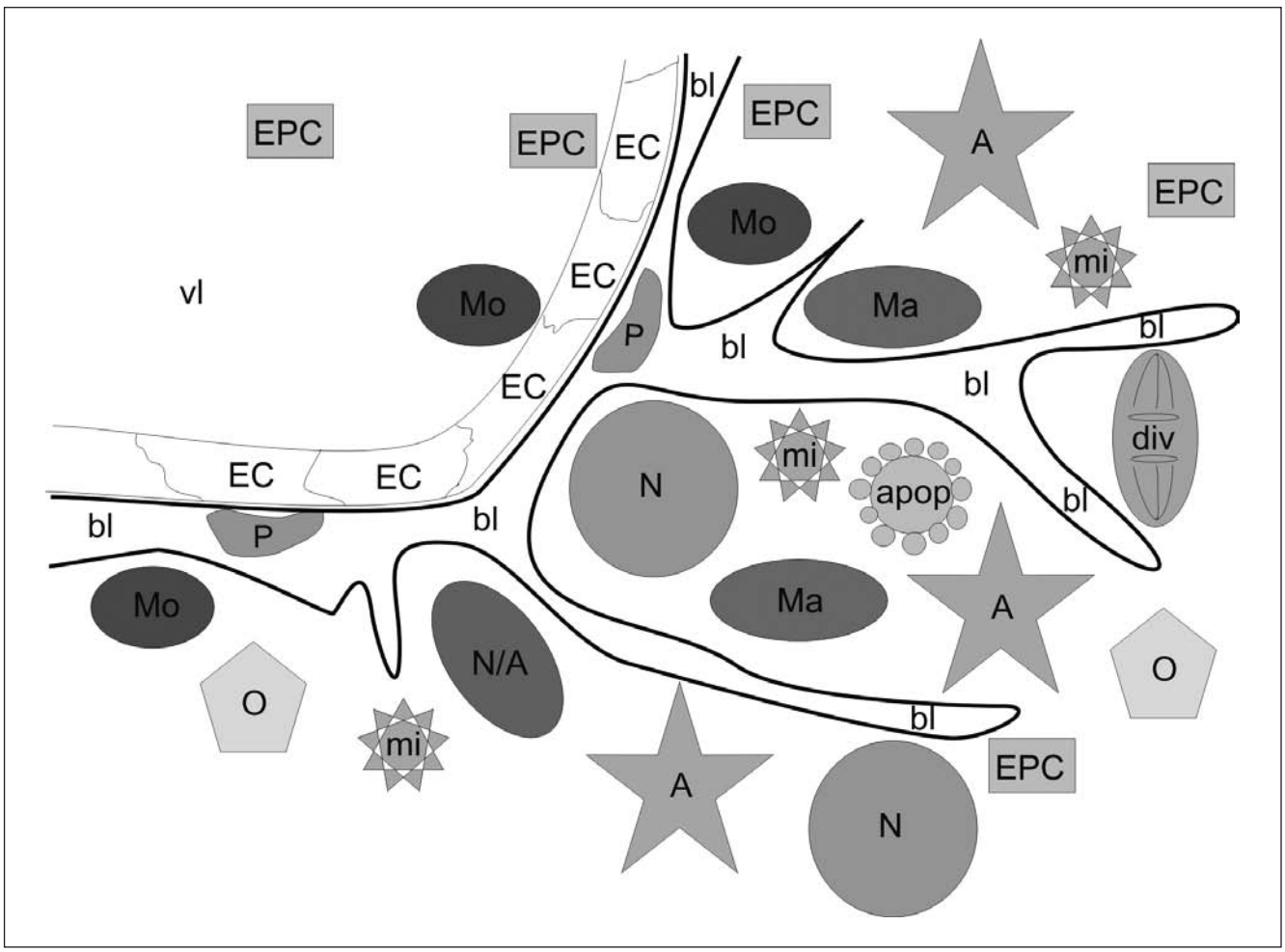

Fig. 12. Scheme of SBI-induced vascular niche. Basal lamina branching results in the development of fractones. A – astrocyte, apop – apoptotic cell, bl – basal lamina, div – dividing cell, EC – endothelial cell, EPC – endothelial progenitor cell, mi – microglial cell, N – neuron, Ma – macrophage, Mo – monocyte, N/A – nestin-positive cell, O – oligodendrocyte, P – pericyte, vl – capillary vessel lumen.

neurovascular units in the injury zone by replacing damaged neurons and glial cells (Romanko et al. 2004), or in the formation of glial scar. They might also act in a paracrine way as the source of trophic factors that promoted healing. However, nestin re-expression can also take place *in situ* (in resident cells) in the adult brain damaged region during formation of the glial scar (Michalczyk and Ziman 2005). Notably, the emergence of a small number of DCX-positive cells in the neocortex after its injury was reported in a mouse model (Susarla et al. 2014). Yet another source of these cells may be NG2-positive mesenchymal stem cells that have neural lineage potential (Okolicsanyi et al. 2014). It was shown that NG2-positive cells proliferate quickly after brain injury (Susarla et al. 2014) and can differentiate into oligodendrocytes that take part in reconstruction of the brain parenchyma (Nishiyama et al. 2009). Many, while not all, researchers indicated also to the potential of these cells for differentiation into both astroglia, synantocytes and neurons depending on the type and extent of the injury, and on the state of its surroundings (Butt et al. 2005, Aguirre et al. 2007, Zhu et al. 2008, Haselkorn et al. 2010, Morrens et al. 2012). It has also been shown that NG2-positive cells affect, at later post-injury times, the formation of glial scar and modulate the ECM structure locally by secreting chondroitin sulphate proteoglycans (Tan et al. 2005, Yi et al. 2012). The latter can exert a negative effect on the healing process by hindering the re-growth of damaged axons in the peri-SBI zone (Rhodes et al. 2003, Butt et al. 2005, Tan et al. 2005).

Studies on the processes induced by brain cortex injury indicate that the cells migrating from the SVZ to the injury site differentiate mostly into glial cells (Chirumamilla et al. 2002, Ramaswamy et al 2005). This observation may help explaining the low number of cells with immature neuron phenotype reported in the peri-injury zone, both in our and in other models of traumatic brain injury (Susarla et al. 2014).

In our material, the phenomena discussed above were associated with massive proliferation and invasion of brain parenchyma by the local basal lamina, forming, inter alia,

branched three-dimensional structures closely resembling those termed fractones (Mercier et al. 2002, 2003, Kerever et al. 2007, 2015). Similar changes associated with the synthesis of the main components of basal lamina and ECM (fibronectin and laminin) were also reported in adult rats 7–21 days after closed cryogenic brain injury (Suzuki and Choi 1990). Those authors suggested that the newly formed basal lamina was made by subpial astrocytes in close interaction with ECM components at the pia surface. In our model, the injury consists in removal of both a piece of neocortex and the overlaying part of meninges. Hence, it is more likely that the proliferation of the basal lamina is mostly the result of action of perivascular astrocytes located deeper in the brain parenchyma.

A question may arise of what comes first after the SBI: the formation of fractone network, or brain cells' proliferation? We cannot answer this question based on the present knowledge. However, the existing body of data strongly suggests that there is a close relationship between the specific structures of perivascular basal lamina and neurogenesis, both under physiological conditions and in emergency situations created by brain insults.

The results of this study demonstrate that SBI results in the formation of a zone of active repair and remodeling at the injury perimeter. The center of the processes described above is the blood vessel, whose basal lamina is connected with of multi-branched three-dimensional structures (fractones). The fractone network that, in the brain, has only been found in classical neurovascular niches, encompasses both terminally differentiated and immature cells of diverse phenotypes, including some dividing cells. The architecture of this zone (for a scheme see Fig. 12) resembles that of other vascular niches (Nikolova et al. 2006) as well of the vascular component of classical neurovascular niches, e.g., of SVZ (Madri 2009). It is known that many cell types participating in post-traumatic remodeling of brain parenchyma require the presence of the basal lamina that cannot be formed by the cells themselves, and it is the role of the vascular niche to provide this specific component for these high plasticity cells (Nikolova et al. 2006). We found no signs of local neurogenesis in the peri-SBI region (including the immediate vicinity of fractone network), which suggests that the identified structure was but a vascular niche. At present, one cannot definitely exclude the possibility that this niche would have become, at later post-SBI times, a home for neuroblasts migrating from a classical neurogenetic niche, e.g., from the SVZ. However, this is rather unlikely because our earlier studies have shown no neurogenesis in the SBI zone between 2 and 24 weeks post-SBI. Whereas one could argue that it could occur between the 4th and 13th post-injury day, it is hard to believe that such a delayed neurogenesis could be accomplished 2 weeks post-SBI, when the remodeling of the injury site is far from finished.

AUTHOR CONTRIBUTIONS

All the authors participated in the design of the study, analysis and interpretation of study results, as well as in writing the manuscript, and accepted the final version of the manuscript.

ACKNOWLEDGEMENT

This study was supported by the National Centre for Research and Development Project NN 404 522838.

REFERENCES

Aguirre A, Dupree JL, Mangin JM, Gallo V (2007) A functional role for EGFR signaling in myelination and remyelination. Nat Neurosci 10: 990–1002.

Alvarez-Buylla A, Garcia-Verdugo JM (2002) Neurogenesis in adult subventricular zone. J Neurosci 22: 629–634.

Butt AM, Hamilton N, Hubbard P, Pugh M, Ibrahim M (2005) Synantocytes: the fifth element. J Anat 207: 695–706.

Carmeliet P (2003) Angiogenesis in health and disease. Nat Med 9: 653–660.

Cheng MF (2013) Hypothalamic neurogenesis in the adult brain. Front Neuroendocrinol 34: 167–178.

Chirumamilla S, Sun D, Bullock MR, Colello RJ (2002) Traumatic brain injury induced cell proliferation in the adult mammalian central nervous system. J Neurotrauma 19: 693–703.

Corselli M, Chen CW, Crisan M, Lazzari L, Péault B (2010) Perivascular ancestors of adult multipotent stem cells. Arterioscler Thromb Vasc Biol 30: 1104–1109.

del Zoppo GJ, Milner R, Mabuchi T, Hung S, Wang X, Berg GI, Koziol JA (2007) Microglial activation and matrix protease generation during focal cerebral ischemia. Stroke 38: 646–651.

Doetsch F (2003) A niche for adult neural stem cells. Curr Opin Genet Dev 13: 543–550.

Domingues AM, Taylor M, Fern R (2010) Glia as transmitter sources and sensors in health and disease. Neurochem Int 57: 359–366.

Dvorak HF, Brown LF, Detmar M, Dvorak AM (1995) Vascular permeability factor/vascular endothelial growth factor, microvascular hyperpermeability and angiogenesis. Am J Pathol 146: 1029–1039.

Fan Y, Yang GY (2007) Therapeutic angiogenesis for brain ischemia: a brief review. J Neuroimmune Pharmacol 2: 284–289.

Frontczak-Baniewicz M, Chrapusta SJ, Sulejczak D (2011) Long-term consequences of surgical brain injury – characteristics of the neurovascular unit and formation and demise of the glial scar in a rat model. Folia Neuropathol 49: 204–218.

Frontczak-Baniewicz M, Walski M (2003) New vessel formation after surgical brain injury in the rat's cerebral cortex I. Formation of the blood vessels proximally to the surgical injury. Acta Neurobiol Exp (Wars) 63: 65–75.

Frontczak-Baniewicz M, Walski M (2006) Glial scar instability after brain injury. J Physiol Pharmacol 57 Suppl 4: 97–102.

Frontczak-Baniewicz M, Walski M, Sulejczak D (2007) Diversity of immunophenotypes of endothelial cells participating in new vessel formation following surgical rat brain injury. J Physiol Pharmacol 58 Suppl 5: 193–203.

Gage FH (2002) Neurogenesis in the adult brain. J Neurosci 22: 612–613.

Gage FH, Kempermann G, Palmer TD, Peterson DA, Ray J (1998) Multipotent progenitor cells in the adult dentate gyrus. J Neurobiol 36: 249–66.

Gu W, Brännström T, Wester P (2000) Cortical neurogenesis in adult rats after reversible photothrombotic stroke. J Cereb Blood Flow Metab 20: 1166–1173.

Halfter W (1998) Disruption of the retinal basal lamina during early embryonic development leads to a retraction of vitreal end feet, an increase number of ganglion cells, and aberrant axonal outgrowth. J Comp Neurol 397: 89–104.

Han RZ, Hu JJ, Weng YC, Li DF, Huang Y (2009) NMDA receptor antagonist MK-801 reduces neuronal damage and preserves learning and memory in a rat model of traumatic brain injury. Neurosci Bull 25: 367–375.

Haselkorn ML, Shellington DK, Jackson EK, Vagni VA, Janesko-Feldman K, Dubey RK, Gillespie DG, Cheng D, Bell MJ, Jenkins LW, Homanics GE, Schnermann J, Kochanek PM (2010) Adenosine A1 receptor activation as a brake on the microglial response after experimental traumatic brain injury in mice. J Neurotrauma 27: 901–910.

Hur J, Yoon CH, Kim HS, Choi JH, Kang HJ, Hwang KK, Oh BH, Lee MM, Park YB (2004) Characterization of two types of endothelial progenitor cells and their different contributions to neovasculogenesis. Arterioscler Thromb Vasc Biol 24: 288–293.

Ito U, Nagasao J, Kawakami E, Oyanagi K (2007) Fate of disseminated dead neurons in the cortical ischemic penumbra: ultrastructure indicating a novel scavenger mechanism of microglia and astrocytes. Stroke 38: 2577–2583.

Jiang W, Gu W, Brännström T, Rosqvist R, Wester P (2001) Cortical neurogenesis in adult rats after transient middle cerebral artery occlusion. Stroke 32: 1201–1207.

Jin K, Sun Y, Xie L, Peel A, Mao XO, Batteur S, Greenberg DA (2003) Directed migration of neuronal precursors into the ischemic cerebral cortex and striatum. Mol Cell Neurosci 24: 171–189.

Kerever A, Schnack J, Vellinga D, Ichikawa N, Moon C, Arikawa-Hirasawa E, Efird JT, Mercier F (2007) Novel extracellular matrix structures in the neural stem cell niche capture the neurogenic factor Fibroblast Growth Factor 2 from the extracellular milieu. Stem Cells 25: 2146–2157.

Kerever A, Yamada T, Suzuki Y, Mercier F, Arikawa-Hirasawa E (2015) Fractone aging in the subventricular zone of the lateral ventricle. J Chem Neuroanat 66–67: 52–60.

Lossinsky AS, Shivers RR (2004) Structural pathways for macromolecular and cellular transport across the blood-brain barrier during inflammatory conditions. Histol Histopathol 19: 535–564.

Madri JA (2009) Modeling the neurovascular niche: implications for recovery from CNS injury. J Physiol Pharmacol 60 Suppl 4: 95–104.

Mercier F, Kitasako JT, Hatton GI (2002) Anatomy of the brain neurogenic zones revisited: fractones and the fibroblast/macrophage network. J Comp Neurol 451: 170–188.

Mercier F, Kitasako JT, Hatton GI (2003) Fractones and other basal laminae in the hypothalamus. J Comp Neurol 455: 324–340.

Michalczyk K, Ziman M (2005) Nestin structure and predicted function in cellular cytoskeletal organisation. Histol Histopathol 20: 665–671.

Morgan R, Kreipke CW, Roberts G, Bagchi M, Rafols JA (2007) Neovascularization following traumatic brain injury: possible evidence for both angiogenesis and vasculogenesis. Neurol Res 29: 375–381.

Morrens J, Van Den Broeck W, Kempermann G (2012) Glial cells in adult neurogenesis. Glia 60: 159–174.

Nag S (2002) The blood-brain barrier and cerebral angiogenesis: lessons from the cold-injury model. Trends Mol Med 8: 38–44.

Nag S (2003) Pathophysiology of blood-brain barrier breakdown. Methods Mol Med 89: 97–119.

Nag S, Manias JL, Stewart DJ (2009) Expression of endothelial phosphorylated caveolin-1 is increased in brain injury. Neuropathol Appl Neurobiol 35: 417–426.

Nag S, Takahashi JL, Kilty DW (1997) Role of vascular endothelial growth factor in blood-brain barrier breakdown and angiogenesis in brain trauma. J Neuropathol Exp Neurol 56: 912–921.

Nikolova G, Strilic B, Lammert E (2006) The vascular niche and its basement membrane. Trends Cell Biol 17: 19–25.

Nishiyama A, Komitova M, Suzuki R, Zhu X (2009) Polydendrocytes (NG2 cells): multifunctional cells with lineage plasticity. Nat Rev Neurosci 10: 9–22.

Ohab JJ, Fleming S, Blesch A, Carmichael ST (2006) A neurovascular niche for neurogenesis after stroke. J Neurosci 26: 13007–13016.

Ohira K, Furuta T, Hioki H, Nakamura KC, Kuramoto E, Tanaka Y, Funatsu N, Shimizu K, Oishi T, Hayashi M, Miyakawa T, Kaneko T, Nakamura S (2010) Ischemia-induced neurogenesis of neocortical layer 1 progenitor cells. Nat Neurosci 13: 173–179.

Okolicsanyi RK, Griffiths LR, Haupt LM (2014) Mesenchymal stem cells, neural lineage potential, heparan sulfate proteoglycans and the matrix. Dev Biol 388: 1–10.

Peichev M, Naiyer AJ, Pereira D, Zhu Z, Lane WJ, Williams M, Oz MC, Hicklin DJ, Witte L, Moore MA, Rafii S (2000) Expression of VEGFR-2 and AC133 by circulating human CD34$^+$ cells identifies a population of functional endothelial precursors. Blood 95: 952–958.

Ramaswamy S, Goings GE, Soderstrom KE, Szele FG, Kozlowski DA (2005) Cellular proliferation and migration following a controlled cortical impact in the mouse. Brain Res 1053: 38–53.

Rhodes KE, Moon LD, Fawcett JW (2003) Inhibiting cell proliferation during formation of the glial scar: effects on axon regeneration in the CNS. Neuroscience 120: 41–56.

Riquelme PA, Drapeau E, Doetsch F (2008) Brain micro-ecologies: neural stem cell niches in the adult mammalian brain. Philos Trans R Soc Lond B Biol Sci 363: 123–137.

Romanko MJ, Rola R, Fike JR, Szele FG, Dizon ML, Felling RJ, Brazel CY, Levison SW (2004) Roles of the mammalian subventricular zone in cell replacement after brain injury. Prog Neurobiol 74: 77–99.

Rosenstein JM, Krum JM (2004) New roles for VEGF in nervous tissue – beyond blood vessels. Exp Neurol 187: 246–253.

Sulejczak D, Grieb P, Walski M, Frontczak-Baniewicz M (2008) Apoptotic death of cortical neurons following the surgical brain injury. Folia Neuropathol 46: 213–219.

Sundholm-Peters NL, Yang HK, Goings GE, Walker AS, Szele FG (2005) Subventricular zone neuroblasts emigrate toward cortical lesions. J Neuropathol Exp Neurol 64: 1089–1100.

Susarla BT, Villapol S, Yi JH, Geller HM, Symes AJ (2014) Temporal patterns of cortical proliferation of glial cell populations after traumatic brain injury in mice. ASN Neuro 6: 159–170.

Suzuki M, Choi BH (1990) The behavior of the extracellular matrix and the basal lamina during the repair of cryogenic injury in the adult rat cerebral cortex. Acta Neuropathol 80: 355–361.

Tan AM, Zhang W, Levine JM (2005) NG2: a component of the glial scar that inhibits axon growth. J Anat 207: 717–725.

Thored P, Arvidsson A, Cacci E, Ahlenius H, Kallur T, Darsalia V, Ekdahl CT, Kokaia Z, Lindvall O (2006) Persistent production of neurons from adult brain stem cells during recovery after stroke. Stem Cells 24: 739–747.

Walski M, Frontczak-Baniewicz M (2003) New vessel formation after surgical brain injury in the rat's cerebral cortex II. Formation of the blood vessels distal to the surgical injury. Acta Neurobiol Exp (Wars) 63: 77–82.

Xu Y, Tamamaki N, Noda T, Kimura K, Itokazu Y, Matsumoto N, Dezawa M, Ide C (2005) Neurogenesis in the ependymal layer of the adult rat 3rd ventricle. Exp Neurol 192: 251–264.

Yamashita T, Ninomiya M, Hernandez Acosta P, Garcia-Verdugo JM, Sunabori T, Sakaguchi M, Adachi K, Kojima T, Hirota Y, Kawase T, Araki N, Abe K, Okano H, Sawamoto K (2006) Subventricular zone-derived neuroblasts migrate and differentiate into mature neurons in the post-stroke adult striatum. J Neurosci 26: 6627–6636.

Yi JH, Katagiri Y, Susarla B, Figge D, Symes AJ, Geller HM (2012) Alterations in sulfated chondroitin glycosaminoglycans following controlled cortical impact injury in mice. J Comp Neurol 520: 3295–3313.

Zhu X, Hill RA, Nishiyama A (2008) NG2 cells generate oligodendrocytes and gray matter astrocytes in the spinal cord. Neuron Glia Biol 4: 19–26.